

General Disclaimer

One or more of the Following Statements may affect this Document

- This document has been reproduced from the best copy furnished by the organizational source. It is being released in the interest of making available as much information as possible.
- This document may contain data, which exceeds the sheet parameters. It was furnished in this condition by the organizational source and is the best copy available.
- This document may contain tone-on-tone or color graphs, charts and/or pictures, which have been reproduced in black and white.
- This document is paginated as submitted by the original source.
- Portions of this document are not fully legible due to the historical nature of some of the material. However, it is the best reproduction available from the original submission.

X-661-75-278

PREPRINT

NASA TM-X 71019

THE ISOTOPIC COMPOSITION OF COSMIC RAYS WITH $5 \leq Z \leq 26$

A. J. FISHER
F. A. HAGAN
R. C. MAEHL
J. F. ORMES
J. F. ARENS

OCTOBER 1975

(NASA-TM-X-71019) THE ISOTOPIC COMPOSITION
OF COSMIC RAYS WITH Z IS LESS THAN OR EQUAL
TO 26 WHICH IS LESS THAN OR EQUAL TO 26

N76-12931

(NASA) 32 p HC \$4.00

CSCI 03E

Unclass

G3/93 04232

GSTC

— GODDARD SPACE FLIGHT CENTER —
GREENBELT, MARYLAND



THE ISOTOPIC COMPOSITION OF COSMIC RAYS WITH ~~5<Z<26~~

A. J. Fisher**, F. A. Hagen*, R. C. Maehl^{**}, J. F. Ormes, J. F. Arens
NASA/Goddard Space Flight Center
Greenbelt, Maryland 20771

*Work supported by NASA Grant 21-002-316

**NAS/NRC Resident Research Associate at GSFC

THE ISOTOPIC COMPOSITION OF COSMIC RAYS WITH $5 \leq Z \leq 26$

ABSTRACT

We report here results obtained from a high altitude balloon flight from Thompson, Canada in August, 1973. The instrument consisted of a spark chamber, a Lucite Cerenkov counter and thirteen layers of scintillators. For heavy particles we use the Cerenkov-range method of analysis to determine the mass of particles energetic enough to produce a Cerenkov signal and then stop in the layered scintillators. In the energy range $350 \text{ MeV/amu} \leq T \leq 600 \text{ Mev/amu}$ we find $^{16}\text{O}/\text{O} > .9$, $^{12}\text{C}/\text{C} > .9$, $^{14}\text{N}/\text{N} = .6 \pm .2$. Additionally we find even-Z elements in the $12 \leq Z \leq 16$ group to be predominantly α -particle nuclei. Neon, on the other hand seems to have a significant component of neutron rich isotopes. While we are limited by statistical accuracy in the $17 \leq Z \leq 25$ region, the data appears to be consistent with current cosmic-ray propagation models. We find iron to be predominantly ^{56}Fe , with some ^{54}Fe being evident, the mean mass of iron calculated from this data is 55.4 ± 0.3 . Using a simple exponential path length propagation model we extrapolate this data to the cosmic-ray source and discuss some implications of the data as to the nature of the source.

I. INTRODUCTION

Studies of the chemical composition of the cosmic radiation have indicated both their surprising similarity to solar system composition as well as significant differences. Many of these differences have been caused in the cosmic ray propagation, but some are probably related to the composition of the source itself. By studying the isotopic composition of the cosmic rays, we may hope to understand these source differences as being related to the conditions under which the cosmic ray nucleo-synthesis occurs.

In order to begin to attack this problem experimentally, we have flown an experiment to measure the isotopic composition using a Cerenkov-range technique in which we have measured the mass of the arriving cosmic rays in the $5 \leq Z \leq 26$ charge region for kinetic energies around 450 MeV/amu. In this paper we present the experimental and data analysis details which we have used to find the isotopic composition.

This comprehensive survey of the cosmic ray masses is combined with the excellent charge composition data from the same balloon flight, from which we derive source chemical and isotopic composition using the most recent spallation cross section data. We then consider some of the possible implications of the data.

II. INSTRUMENT AND EVENT SELECTION

Measuring the isotopic composition of cosmic rays is an extremely challenging task. It means measuring the charge to mass ratio to accuracies of a few percent. This requires either bending the particle in a magnetic field or stopping (or significantly slowing) the particle. We have used the latter technique on a balloon borne experiment flown from Thompson, Canada in August 1973.

The instrument, shown in Fig. 1, consists of a spark chamber, a Lucite Cerenkov counter and several layers of scintillators. The spark chamber consists of eight grids in both the X and Y dimensions which produce a digitized readout from which we determine the zenith angle to better than one half degree accuracy. Using the zenith angle, the two top scintillators (S1 and S2) and the Cerenkov counter we determine the charge of each event. The details of this analysis are presented elsewhere (Ormes et al., 1975). The charge resolution is quite good, $\sigma \sim 0.1$ charge unit at oxygen, so we have unambiguous charge identification. In order to achieve such good charge resolution we have mapped all of our detectors as a function of position, zenith angle and time drifts to a uniformity within 1%.

Once we know the charge, we determine the velocity, β (where $\beta = v/c$) from the Cerenkov counter using the method described in section III below.

In order for an event to be considered for analysis in the Cerenkov-range mode it must meet three criteria: It must be above the Cerenkov threshold throughout the Lucite ($T_{th} = 320$ MeV/amu), it must stop in one of the scintillators below the Cerenkov counter and it must not undergo a nuclear interaction. The first of these criteria limits us to events with $Z \geq 5$, since for $Z < 5$ and, in fact, for almost all events with $Z = 5$, particles sufficiently energetic to give a Cerenkov signal have ranges longer than our stack thickness. The second and third criteria are coupled as follows: since dE/dx increases as the particle slows down, we require the relative pulse heights of the scintillators to increase as the particle penetrates more deeply into the stack (allowing for statistical variations in dE/dx). When we find a pulse-height that decreases,

but is still non-zero, we label that scintillator as the stopping detector. Criterion two is satisfied by tracing the spark chamber trajectory to insure the particle has not left the stack at this point. The third criterion is met by requiring all detectors below the stopping detector to have pulse heights below the level of a minimum ionizing singly-charged particle. This works because any interaction product is lighter and therefore has a longer range than its progenitor. This criterion detects even interactions which strip off only a single proton. In fact, this criterion will detect neutron stripping reactions if the fast neutron n, p scatters in the lower scintillators; however, the efficiency of detecting such events is not high.

Due to the low but non-zero noise level, the interaction criterion becomes somewhat less reliable near the bottom of the stack; therefore, events that stop in S-12 and S-13 are not included in the analysis (with the exception of boron where S-12 is included, since all of our boron sample stops in S-12 and S-13). As a practical matter, these two detectors are relatively unimportant to the mass analysis since most events with such a long range (essentially all the events with $Z \geq 10$) undergo a nuclear interaction before stopping. Therefore, the great majority of the events which stop in S-12 and S-13 intact are C, N, and O; and since we are not statistically limited for these elements, eliminating these events does no harm and prevents a bias toward heavier mass (due to increased range) which comes with such interactions.

III. MASS DETERMINATION

Once an event has passed all the acceptance criteria we wish to find the mass. Given the range and β the expression for A is

$$A = Z^2 R_{Z,A} / R_{1,1}(\beta) \quad (1)$$

where $R_{Z,A}$ is the range measured for the event and $R_{1,1}(\beta)$ is the equivalent proton range at the velocity β as determined from the range-energy tables (Barkas and Berger, 1964). The range of the particle which stops in our detector is measured from the middle of the Cerenkov counter by knowing the scintillator thicknesses (to 25 microns), the zenith angle (as discussed above) and the pulse heights in the stopping detector (k) and the one above it ($k-1$). The range energy relationship can be written

$$R = \bar{K} \frac{A}{Z^2} (E/A)^\gamma, \quad (2)$$

where \bar{K} and γ are only weakly dependent on R and Z . One can show that ΔR , the range in detector k , is related to the energy deposit in detector k (E_k), the energy deposit in detector $k-1$ (E_{k-1}) and the thickness of detector $k-1$ (t_{k-1}) by

$$\Delta R = \sec \theta t_{k-1} \left[\frac{1}{(E_{k-1}/E_k + 1)^{\gamma} - 1} \right], \quad (3)$$

independent of Z and A , provided γ is independent of Z and R . We can determine γ from particles which stop near scintillator boundaries, i.e. particles for which the range is well known. We find

$$\gamma = \frac{\ln(t_{k-1}/t_k + 1)}{\ln(E_{k-1}/E_k + 1)} \approx 1.3 \quad (4)$$

The procedure for determining the velocity can best be discussed by reference to Fig. 2. The Cerenkov response is made of three components: (1) the classical Cerenkov radiation

$$C = \bar{K} Z^2 (1 - 1/\beta^2 n^2), \quad (5)$$

(2) the Cerenkov radiation due to the delta rays produced by the ionization loss of the particle (which varies differently with β than the Cerenkov radiation produced directly by the particle) and (3) the residual scintil-

lation light from the Lucite.

We determine the β dependence of the scintillation light by considering the events, below the Cerenkov threshold, for which we can determine velocity from the range and the range-energy tables. The data shown in Fig. 2 is for carbon nuclei, we have assumed for this purpose ^{12}C . Doing this, we reconstruct the data points in Fig. 2, the total Cerenkov response vs. β . Below the threshold (nominally $n = 1.49$, $\beta_{th} = 0.67$) the response is due primarily to residual scintillation, this determines the fraction of scintillation light as a function of β as shown. The shape fits well to the velocity dependence of our plastic scintillators, i.e. appears to have the same saturation properties. Therefore, we use the average of the two scintillation pulse heights of each event, to determine the residual scintillation contribution to the pulse height. The normalization constant is determined by the response in the $\beta < 0.67$ region. The response for our particular detector is somewhat flatter as a function of β than an unsaturated scintillation response and predicts a higher fraction of the pulse height due to residual scintillation at $\beta=1$ than assumed by Lezniak (1975) in his recent paper on the response of Cerenkov detectors.

The response due to delta rays is calculated based on a finite cutoff energy corresponding to particles whose range equals the thickness of the Cerenkov detector. The number of delta rays is known to go as Z^2 and the β dependence comes directly from the calculation. The δ ray contribution to the Cerenkov light emission is thus calculated uniquely relative to the classical Cerenkov emission for all charges. The sum of these three components gives the total Cerenkov signal in a form directly comparable to the pulse height.

The final parameter we need to know is the location of the $\beta=1$ pulse height, $C_{\max}(Z)$, this is determined following the procedure out-

lined by Leznik (1975). Using this procedure we can check that the response is proportional to Z^2 . From the three-component response curves, the Cerenkov signal and $C_{\max}(Z)$, β can be calculated. Using the range energy tables of Barkas and Berger (1964) the proton range $R_{1,1}(\beta)$ is then determined.

All the parameters in (1) are now fixed so the mass is also fixed for each event with no arbitrary normalization. Figure 3 shows the mass resolution as a function of C/C_{\max} as derived from laboratory calibration data (muons). For events with $Z > 10$ where photo-electron statistics are no longer the only dominant resolution effect, the resolution does not improve as fast as Z^{-1} .

We wish to emphasize that the mass scale is determined by the range at which a particle begins to emit Cerenkov radiation, and this is very insensitive to the previous arguments. For example, if the $C_{\max}(Z)$ point is misidentified, or if the relative amount of scintillation light is incorrect, the masses determined will be a function of the range of the particles. This internal check makes the method very powerful and is used to estimate the size of possible residual systematic errors.

IV. RESULTS

Figure 4 shows some of the mass histograms which result from this analysis. Note that there are two nuclei with only one long-lived isotope ^{19}F and ^{23}Na . These two elements verify our argument of the previous section that what we derive is in fact an absolute mass and no arbitrary normalization assumptions are necessary. For both F and Na we find Gaussian distributions centered on exactly ^{19}F and ^{23}Na with resolution compatible with single isotope distributions. This fact, coupled with a careful analysis of possible systematic errors leads us to conclude that the residual systematic error in the mass scale is < 0.2 amu over the entire range of $5 \leq Z \leq 26$ and for most elements < 0.1 . These residual uncertainties are due to residual uncertainties in the precise location of the $\beta=1$ Cerenkov position and the extrapolation of the β dependence of the scintillation is the Lucite from the region of $\beta < 0.67$ to the region with $\beta > 0.67$.

In table 1a and 1b we show results from these distributions. Table 1a shows the mean masses calculated for the data. We use mean masses since for many of the elements the statistical accuracy does not warrant analytical peak fitting methods to extract individual isotope abundances. Along with our results in table 1a are the data of Webber (1971) measured by a dE/dX -E-Range analysis and the data of Webber et al (1973) measured by Cerenkov-Total E. All the data are in essential agreement, in the latter case we have computed a mean mass from quoted abundances. Webber claims a residual uncertainty of ± 0.5 amu in the absolute mass normalization. In table 1b we present more detailed results for the more abundant elements. We have fitted a series of Gaussian distributions to the nuclei that have sufficient statistical accuracy to merit such a fit. Note that in fitting these peaks the positions of the various isotopes are known and therefore not allowed to vary. The mass resolution is varied to minimize χ^2 , we find $\chi^2_{\text{Reduced}} \sim 0.7$ for all these elements so the fits are quite good. The errors represent statistical and possible systematic errors as well as uncertainties due to the peak-fitting of the data (this effect is significant only for nitrogen). These data will be discussed in more detail below.

V. PROPAGATION THROUGH THE GALAXY

Since we are ultimately interested in the isotopic composition at the cosmic-ray source, we need to account for propagation effects in the galaxy. In order to do this we have adopted a simple exponential path

length model, in which the interstellar medium is assumed to be 90% H and 10% He. The spallation cross sections used in this calculation are from the semi-empirical formula of Silberberg and Tsao (1973a, 1973b). The calculation is done on an isotope by isotope basis, all short-lived isotopes are allowed to decay. We use a leakage length of 6.0 g/cm^2 based on the fit of secondary/primary ratios and a source composition which fits chemical composition data from the same flight. (Ormes et al., 1975; Maehl et al., 1975). These data will be described more extensively in a following paper but are in general in essential agreement with previously published estimated of the cosmic ray source composition (Shapiro et al., 197^a) based on a similar propagation model.

Since the isotopic measurements considered here are for 350 MeV/amu $\leq T \leq 600$ MeV/amu we assume a representative energy of ~800 MeV/amu (the particles lose 200 to 400 MeV/amu in entering the solar cavity from interstellar space) as the value used in the calculation of the cross sections. Although the chemical composition is somewhat energy dependent, especially for $Z > 15$ (Maehl et al. 1975), the relative isotopic composition of the secondaries is essentially energy independent (above a few hundred MeV/amu). Thus the precise value of the energy used in the calculation of the cross sections is not critical for isotopic measurements. Note also that the isotopic composition is also only weakly dependent on uncertainties in leakage length. Except where specifically noted below we consider the isotopic distribution of the nuclei at the source to be the same as the solar system abundances of Cameron (1973).

In Table 11 we show the predicted and observed chemical isotopic composition of the arriving cosmic rays. The derivation of the chemical composition from the data and the procedure for the extrapolation to the top of the atmosphere will be considered in a later paper.

VII. ISOTOPIC COMPOSITION $6 \leq Z \leq 8$

In this charge region we find the source isotopic composition to be predominantly nuclides with $A/Z = 2.0$. Table 1b shows the result of the propagation calculation on an isotope by isotope basis for these elements with the data also given in such a form. The upper limits on ^{13}C and ^{17}O are on the order of 50% above the values expected on the basis of the propagation model if these nuclides are absent at the source. The observations of finite amounts of ^{15}N and ^{18}O are quite consistent with production during propagation. In fact we both predict and observe almost as much ^{18}O ($^{18}\text{O}/\text{C} = 0.023$) as ^{19}F ($^{19}\text{F}/\text{C} = 0.028$), consistent with the absence of both of these constituents at the source at the 0.5% level relative to carbon. Summarizing we find C, N and O to be consistent with pure ^{12}C , ^{14}N and ^{16}O sources, as the observed ^{13}C , ^{15}N , ^{17}O and ^{18}O can be explained in terms of the propagation model. However, on the basis of the current data we cannot rule out trace amounts of these isotopes at the source, consistent, for example, with the universal abundances of Cameron (1973). Note that the nitrogen results are in good agreement with the recent measurements at higher energy (~ 1 GeV/amu) of the nitrogen mean mass by Dwyer and Meyer (1975) of 14.45 ± 0.08 using the geomagnetic cutoff method.

The data also is in agreement with the earlier measurements by Kristiansson et al (1969) who found $^{13}\text{C}/\text{C} \leq 0.15 \pm 0.06$ based on nuclear

emulsion data. They thought their large peak must be due to ^{12}C based on observed tail at the next higher mass. This follows from the prior knowledge that ^{12}C and ^{13}C should be the only carbon isotopes arriving in the cosmic rays. Based on this reasoning they conclude that the cosmic ray source may not be any object in which ^{13}C is copiously produced. The current data with its improved upper limit and its absolute mass normalization can strengthen that conclusion. We can say definitively, based on our detector response above, that the main carbon peak is at ^{12}C . We can further generalize their conclusion to say that the cosmic ray source cannot be any object in which ^{15}N , ^{17}O and ^{18}O is anomalously high.

VIII. ISOTOPIC COMPOSITION $9 \leq Z \leq 16$

A more interesting comparison between the cosmic rays and the universal abundances is found in the $9 \leq Z \leq 16$ region. As previously stated, the monoisotopic elements ^{19}F and ^{23}Na fall in this region along with Ne, Mg, Al and Si. In Table III the measured mean masses of Ne, Mg and Si are shown along with our predictions of the mean masses of the arriving cosmic rays for two cases; (1) assuming the source isotopic composition is the same that is in the solar system and (2) assuming the source of these elements is composed only of isotopes of even Z nuclei with $A/Z = 2.0$. Notice that Mg is the best element to use to differentiate between these two cases since the difference is somewhat larger than the current experimental error. It is high in neutron rich components in the universal abundances ($^{24}\text{Mg} : 25\text{Mg} : 26\text{Mg} = .8 : 1 : .1$) which leads to a mass difference between the two cases of about 0.3 amu after propagation.

In the case of the other elements the differences are smaller. For silicon the universal abundances of ^{28}Si , ^{29}Si and ^{30}Si are .9, .05, and .05 respectively. Neon, on the other hand, has a larger mass difference with $^{22}\text{Ne}/\text{Ne} \sim 10\%$, but this effect is to a large extent subdued in propagation due to the relatively abundant Mg and Si fragmenting into Ne.

If we compare the data in Table III with the predictions we find Si to be consistent with either case but Mg seems to require some neutron-rich component at the source (which is compatible with the solar system abundances). On the other hand, Ne appears to require a source isotopic composition that is even more neutron-rich than the universal abundances. Our best fit to the cosmic-ray source gives $^{20}\text{Ne}/\text{Ne} \sim 0.6$ whereas 90% of the solar system is ^{20}Ne . Recall from table I that the previous measurement of Webber (1971) based on the normalization assumption of $0 = 16.00\text{amu}$ shows similar results. We have previously argued (Maehl et al., 1975) that the uncertainties in the cross sections used in the propagation calculations are unlikely to be large enough that this could be some propagation effect. It is more likely that there is considerable neutron rich Ne is in fact ^{currently accepted} present at the source. Assuming the/isotopic composition of Ne in the solar system is correct, the cosmic ray source neon is considerably more neutron rich than the solar system material. This may provide some new insight to the physical properties of the source and/or cosmic-ray nucleosynthesis.

The Al data is interesting since it may provide us with "nuclear clock" for determining the age of cosmic rays by means of ^{26}Al , $t_{1/2} \sim 7.5 \times 10^5$ years. The problem with this "nuclear clock" is simply that

^{27}Al is present at the source and also copiously produced in propagation so that even if all the ^{26}Al produced in propagation survives it only comprises 20% of the arriving flux ($\bar{A} = 26.8$). Therefore, the difference between complete ^{26}Al survival and complete ^{26}Al decay is only 0.2amu in the mean mass of the arriving cosmic rays. Additionally, if the cosmic rays are more than 10^3 years old, the minimum age based on the Be data, (Hagen et al., 1975) not very much of the ^{26}Al would survive. Therefore, in order to determine a cosmic-ray age from the Al data it will be necessary to measure the relative isotopic composition to much better than 10% accuracy (preferably 1%), a goal which is clearly out of reach of the present data. Even though the statistical uncertainties are large, both these data and those of Webber et al. (1973) indicate that it may be possible that some of the ^{26}Al survives. If some ^{26}Al is present in the cosmic rays the consequences may be quite interesting. If the ^{26}Al age is significantly less than the ^{10}Be age this would imply that there must be two different sources, one for the elements around oxygen and a near-by source for the iron group, consistent for example with the model suggested by Ramaty et al. (1973) based on differences in energy spectra for $T > 10$ GeV/amu.

An age difference would allow us to distinguish the case where the "two sources" are different regions in the same object from the case where the "two sources" are entirely different objects (this may include the same type of object in different stages of evolution). Therefore, the indication of the possibility of some ^{26}Al survival implies that it is

very important to make more detailed high resolution and statistically accurate measurements of the Al isotopic composition as more data on the ^{10}Be age becomes available.

IX. ISOTOPIC COMPOSITION $16 \leq Z \leq 25$

In the region of $Z > 14$ implications of the data become somewhat uncertain due to the lack of statistics, in the case of the rare odd-Z particles; P, Cl, K, Sc, V and Mn where the statistics are extremely limited and atmospheric effects are quite severe and uncertain, we do not attempt to compute even a mean mass. What we can say in this region is the source sulfur is predominantly ^{32}S and the calcium appears consistent with a source (the Ca is about 50% primordial) that is largely ^{40}Ca . However, as in the case of the $6 \leq Z \leq 8$ group, it is not possible with the current data to distinguish between a source which is pure ^{32}S and ^{40}Ca and a source that has trace amounts of neutron-rich sulfur and/or calcium. As far as the rest of the elements in this charge range are concerned we can only say the data are consistent with the wide mass ranges of the spallation products predicted by the propagation models.

X. SOURCE COMPOSITION $26 \leq Z$

The importance of the isotopic composition of the cosmic-ray iron cannot be over-stated. As Woosley (1975) has pointed out, it directly yields information about the cosmic-ray nucleosynthesis. The resolution and statistical accuracy of the current data is not sufficient to detail the precise composition of the iron at the cosmic-ray source.

However, there are some things which we can say from our data, since our mass scale is absolutely normalized, the mass histogram in Fig. 4 shows that the majority of Fe is ^{56}Fe with the possibility that some ^{54}Fe is present. We find $^{56}\text{Fe}/\text{Fe} \geq 0.6$ with the majority of the rest of the iron having $A \leq 56$. Note that ^{55}Fe decays only in the atomic form since κ -capture is the only decay mode energetically possible. Any ^{55}Fe which may possibly be present at the source in a state stripped of electrons or which is created during propagation will survive. From Fig 4 we also see that very little, if any, of the iron has $A > 56$, specifically we find $^{58}\text{Fe}/\text{Fe} < 0.1$. This result is different from that of Webber et al. (1973) whose results show about equal numbers of ^{54}Fe , ^{56}Fe and ^{58}Fe . If we compare the iron data with what is expected from propagation we find the cosmic ray source may be somewhat enriched in ^{54}Fe (this conclusion must be approached cautiously, however, because the uncertainties in the atmospheric production of ^{54}Fe from ^{56}Fe are quite large). If confirmed by future experiments a slight ^{54}Fe enhancement over the solar system (with ^{56}Fe dominating) would be indicative of a source region somewhat more neutron-rich than the site responsible for the nucleosynthesis responsible for the solar system material (Woosley, 1975). However, as Woosley (1975) points out, the interpretation of the $^{54}\text{Fe}/^{56}\text{Fe}$ ratio in terms of neutron excess at the source depends upon whether the ^{56}Fe is synthesized directly as ^{56}Fe or as ^{56}Ni which subsequently decays. One way to remove this ambiguity is to have some estimate of the $^{60}\text{Ni}/^{58}\text{Ni}$ ratio (Woosley, 1975).

However, the problem of measuring Ni isotopes is extremely difficult. This is primarily due to the fact that $\text{Ni}/\text{Fe} < 0.05$. In the present data we have only three non-interacting Ni events; their masses are 57.8, 58.9 and 57.8. If most of the Ni in cosmic rays is in fact ^{58}Ni , then we can conclude the ^{56}Fe was produced from the decay of ^{56}Ni .

XI. DISCUSSION

Before considering the apparent anomalies in the cosmic-ray isotopes with respect to the solar system it is worth emphasizing that at the level of the current measurements most of the elements have isotopic compositions remarkably similar to the solar system. This implies that even though the specific masses, ages and other possible parameters of the respective sources are different and imply somewhat different compositions, the nuclear physics of the reactions is what determines the major features of the charge and isotopic composition of both sets of matter so for the most part they are qualitatively similar. However, as has been pointed out (Reeves, 1973) this generalization must be approached cautiously, in fact the data do show fundamental differences. The point to be made in considering this similarity is that the cosmic ray isotopic composition is not different enough to require the invocation of some exotic processes of nucleosynthesis. Instead, it appears as if the fundamental nuclear physics which governed the synthesis of the solar system material is also responsible for the cosmic rays which implies the solar system is probably an /^{average} sample of galactic matter.

With this in mind let us consider the differences between the two sets of material.

The neutron-rich Ne and the relative over-abundance of ^{54}Fe are probably unrelated phenomena because the two groups are synthesized at very different temperatures at different zones in the source. The Ne is most likely synthesized by hydrostatic nitrogen burning in a helium zone Howard et al. (1971) or in a hot CNO process at about 10^8°K (Audouze, 1973). The iron is created only when $T > 10^9\text{°K}$ (Clayton & Woosley, 1974), a situation which exists only in the inner parts of the star in late stages of evolution. This temperature is high enough to destroy neon.

The reactions which produce neutron rich isotopes in the $Z \sim 10$ range occur based on the products of the CNO cycle as seed nuclei in regions with $T > 10^6\text{°K}$. This can happen if the star is large enough to allow for convective mixing to bring these seed nuclei out near the surface of the star where these reactions can take place or it can happen in normal hydrogen burning if these nuclei are present during the initial formation of the star. This second alternative is quite interesting, since the cosmic rays may be quite a young sample of matter, 10^6 - 10^7 years since acceleration. If we associate the object that synthesized the cosmic rays with the acceleration mechanism (as opposed to the acceleration of ambient matter) which may be reasonable based on the relative over-abundance of heavy cosmic rays, then we can assume that the cosmic-ray nucleosynthesis was completed shortly before acceleration. If we further assume that the cosmic-ray source is a massive star which evolves quite

quickly then we conclude that this star was initially composed of a more highly evolved sample of matter within the galaxy than was the source responsible for the solar system nucleosynthesis. If this were the case it would be natural to assume the star condensed with a higher mass fraction of the CNO group than the solar system source and this may have provided the seed nuclei necessary to produce the observed neutron rich neon. If this is true the neutron rich component in the $10 \leq Z \leq 14$ region may be due to one of the initial parameters of the source not something created during its evolution.

The Fe group, on the other hand, provides a direct source of information about the nuclear processes which are occurring near the core of the star. It appears from the data that most of the Fe is ^{56}Fe but ^{54}Fe may be present in quantities somewhat greater than in the solar system. This may be due to the source being of slightly different mass or higher initial metallicity than the solar system source (Woosley, 1975) but it requires no exotic nucleosynthetic mechanism.

It is important to realize that these are only possibilities which we are suggesting and until we improve on the statistics and the energy range of the cosmic-ray isotope measurements no definitive conclusions as to the nature of the source are possible. However, based on the current data certain observations are possible. It has been suggested (Cassett and Goret, 1973; Havnes, 1973; Kristiansson, 1975) that the composition

of the cosmic rays at the source is the same as the composition of the solar system and the differences in the chemical composition we observe, after accounting for propagation effects, are due to atomic properties of the matter, such as ionization potential or ionization cross-section, which cause selective acceleration effects.

If we find that the isotopic composition of the cosmic rays at the source is different from the solar system material then the hypothesis that the only differences are caused by selective acceleration mechanisms governed by atomic properties cannot hold. Specifically, the data does not rule out such preferential acceleration effects but it does say the differences in the samples of matter are more fundamental. This statement is based primarily on the neutron rich neon isotopes and the apparent relative overabundance of ^{54}Fe in the cosmic rays with respect to the solar system. While we believe that this experiment represents an important step forward in our understanding of the cosmic ray isotopic composition we also feel that further experiments in this area are important. The differences of the cosmic ray isotopic composition from solar system values are extremely important and should be confirmed by experiments with better resolution, preferably outside the earth's atmosphere. When well understood, the isotopic composition will tell us much about the conditions at the sites of cosmic ray nucleosynthesis.

Figure Captions

Figure 1. Schematic diagram of the detector system. S1, S2, the cerenkov radiator and the spark chamber are used to determine charge and velocity. Range is determined by the method described in the text for those particles which stop between S4 and S13.

Figure 2. Contributions of the classical cerenkov response from the particle, residual scintillation in the Lucite and cerenkov light due to delta rays as a function of β . Those three components comprise the observed cerenkov signal.

Figure 3. The effect of velocity resolution on mass resolution (σ_A) as a function of C/C_{\max} , i.e. β , for the Lucite cerenkov counter.

Figure 4. Mass histograms resulting from this analysis for those elements with sufficient statistics to warrant presentation. For the more abundant elements histograms are also shown grouped by stopping detectors (D1 = S1, D2 = cerenkov, D3 = S2, etc.) Note that in the cases of D-12 and D-13 the mass histograms are broadened and shifted up due to the failure of the criteria to detect nuclear interactions (see text).

PRECEDING PAGE BLANK NOT FILMED

REFERENCES

Audouze, J., 1973, Proc. Conf. on Explosive Nucleosynthesis, Austin, 1, 47.

Barkas, W. H. and M. J. Berger, 1964, NASA SP 3013.

Cameron, A. G. W., 1973, Proc. Conf. on Explosive Nucleosynthesis, Austin 1, 3.

Casse, M. and P. Goret, 1973, Proc. 13th Int. Conf. Cosmic Rays, Denver 1, 584.

Clayton, D. D. and S. E. Woosley, 1974, Rev. Mod. Phys., 46, 755.

Dwyer, R. and P. Meyer, 1975, Phys. Rev. Lett. 35, 601.

Fisher, A. J., J. F. Ormes, and F. A. Hagen, 1973, Proc. 13th Int. Conf. Cosmic Rays, Denver 4, 2895.

Fisher, A. J., F. A. Hagen, R. C. Maehl and J. F. Ormes, 1975, Proc. 14th Int. Conf. Cosmic Rays, to be published.

Hagen, F. A., A. J. Fisher, J. F. Ormes and J. F. Arens, 1975, 14th Int. Conf. Cosmic Rays, to be published.

Hainebach, K. L., D. D. Clayton, W. D. Arnett, S. E. Woosley, 1975, Ap. J. 193, 157.

Havnes, O., 1973, Astron. & Astrophys. 24, 435.

Howard, W. M., W. D. Arnett and D. D. Clayton, 1971, Ap. J., 165, 495.

Kristiansson, K., G. Jonsson and L. Malquist, 1969, Proc. 11th Int. Conf. Cosmic Rays, Budapest.

Kristiansson, K., 1975, Astrophys. & Sp. Sci. 30, 417.

Kulsrud, R. M., J. P. Ostriker and J. E. Gunn, 1972, Phys. Rev. Letters 28, 636.

Lezniak, J. A., 1975, NIM, to be published.

Lindstrom, P. J., D. E. Greiner, H. H. Heckman, B. Cork and F. S. Bieser, 1975, preprint.

Maehl, R. C., F. A. Hagen, A. J. Fisher, and J. F. Ormes, 1975, Proc.

14th Int. Conf. Cosmic Rays, to be published.

Ormes, J. F., A. J. Fisher, F. A. Hagen, R. C. Maehl, and J. F. Arens,

1975, 14th Int. Conf. Cosmic Rays, to be published.

Ramaty, R., V. K. Balasubrahmanyam and J. F. Ormes, 1973, Sci. 180, 731.

Reeves, H., 1973, Proc. 13th Int. Conf. Cosmic Rays, Denver 5, 3323.

Schramm, D. and W. D. Arnett, 1974, Ap. J. Letters 184, L47.

Shapiro, M. M., R. Silberberg, C. H. Tsao, 1973, Proc. 13th Int. Conf.

Cosmic Rays, Denver 1, 578.

Silberberg, R. and C. H. Tsao, 1973a, Ap. J. 25, 315.

Silberberg, R. and C. H. Tsao, 1973b, Ap. J. 25, 335.

Webber, W. R., J. A. Lezniak, and J. Kish, 1973, Proc. 13th Int. Conf.

Cosmic Rays, Denver 1, 120.

Webber, W. R., 1971, Symposium on the Isotopic Composition of the Primary

Cosmic Radiation, P. M. Dauber, editor, Lyngby Denmark, 12.

Woosley, S. E., 1975, preprint.

TABLE Ia

<u>ELEMENT</u>	<u>OBSERVED</u>	<u>WEBBER</u>	<u>WEBBER et al.</u>
	<u>A</u>	<u>(1971)</u>	<u>(1973)</u>
B	10.6 <u>±</u> .2	10.82 <u>±</u> .10	
C	12.05 <u>±</u> .05	12.08 <u>±</u> .07	
N	14.40 <u>±</u> .20	14.65 <u>±</u> .08	
O	16.08 <u>±</u> .05	16.00*	
F	19.0 <u>±</u> .3		
Ne	20.8 <u>±</u> .1	21.07 <u>±</u> .12	
Na	23.0 <u>±</u> .3		
Mg	24.3 <u>±</u> .1	24.25 <u>±</u> .14	24.1
Al	26.6 <u>±</u> .3		26.8
Si	28.1 <u>±</u> .1	28.08 <u>±</u> .14	28.1
S	32.1 <u>±</u> .3		32.1
Ar	36.6 <u>±</u> .6		37.6
Ca	41.6 <u>±</u> .5		42.5
Ti	46.2 <u>±</u> .5		48.2
Cr	51.7 <u>±</u> .6		51.9
Fe	55.4 <u>±</u> .3		56.2

*Normalization Assumption

TABLE 1b

χ^2 FIT RESULTS	SOURCE ^{12}C , ^{14}N , ^{16}O
<u>DATA</u>	<u>PROPAGATION PREDICTIONS</u>
$^{12}\text{C}/\text{C} \geq .91$	$^{12}\text{C}/\text{C} = .94$
$^{13}\text{C}/\text{C} \leq .09$	$^{13}\text{C}/\text{C} = .06$
$^{14}\text{N}/\text{N} = .6 \pm .2$	$^{14}\text{N}/\text{N} = .58$
$^{15}\text{N}/\text{N} = .4 \pm .2$	$^{15}\text{N}/\text{N} = .42$
$^{16}\text{O}/\text{O} \geq .91$	$^{16}\text{O}/\text{O} = .95$
$^{17}\text{O}/\text{O} \leq .065$	$^{17}\text{O}/\text{O} = .025$
$^{18}\text{O}/\text{O} = .075 \pm .015$	$^{18}\text{O}/\text{O} = .025$

TABLE II

ELEMENT	COMPOSITION	OBSERVED A	SOURCE** COMPOSITION	PROPAGATED CHEM. COMPOSITION		PREDICTED A (800 MeV/N)
				2300 MeV/N	800 MeV/N	
Li				.207	.179	6.46
Be	.090±.006	7.84±.06*		.111	.102	8.02
					(.086)	(7.65)
B	.291±.005	10.6 ±.2		.255	.275	10.69
					(.291)	(10.66)
C	1.00	12.05±.05	1.00	1.00	1.00	12.06
N	.300±.005	14.40±.2	.15	.289	.301	14.37
O	.940±.010	16.08±.05	1.09	.939	.932	16.06
F	.028±.002	19.0 ±.3		.022	.023	19.00
Ne	.160±.005	20.8 ±.1	.15	.163	.163	20.47
Na	.042±.002	23.0 ±.3	.02	.034	.035	23.00
Mg	.200±.008	24.3 ±.1	.23	.190	.189	24.38
					(.194)	(24.43)
Al	.036±.001	26.6 ±.3	.025	.035	.035	26.85
					(.030)	(27.00)
Si	.140±.002	28.1 ±.1	.19	.141	.139	28.18
P	.011±.002		.008	.0094	.0093	31.00
S	.032±.001	32.1 ±.3	.03	.029	.029	32.48
Cl	.007±.001			.0063	.0070	35.75
					(.0047)	(35.63)
Ar	.012±.002	36.6 ±.6	.007	.011	.012	37.25
					(.014)	(37.07)
K	.007±.003			.0050	.0065	39.77
Ca	.021±.001	41.6 ±.5	.017	.017	.021	41.43
Sc	.004±.002			.0023	.0036	45.00
Ti	.014±.001	46.2 ±.5		.010	.017	47.17
V	.005±.002			.0053	.0093	49.56
Cr	.015±.001	51.7 ±.6	.003	.010	.018	51.58
Mn	.012±.001		.002	.007	.011	53.87
Fe	.078±.002	55.4 ±.3	.15	.080	.080	55.81

*Be data from the dE/dx-E analysis from agen et al., 1975

**Relative isotopic composition at the source assumed to be the same as the universal abundances (Cameron, 1973)

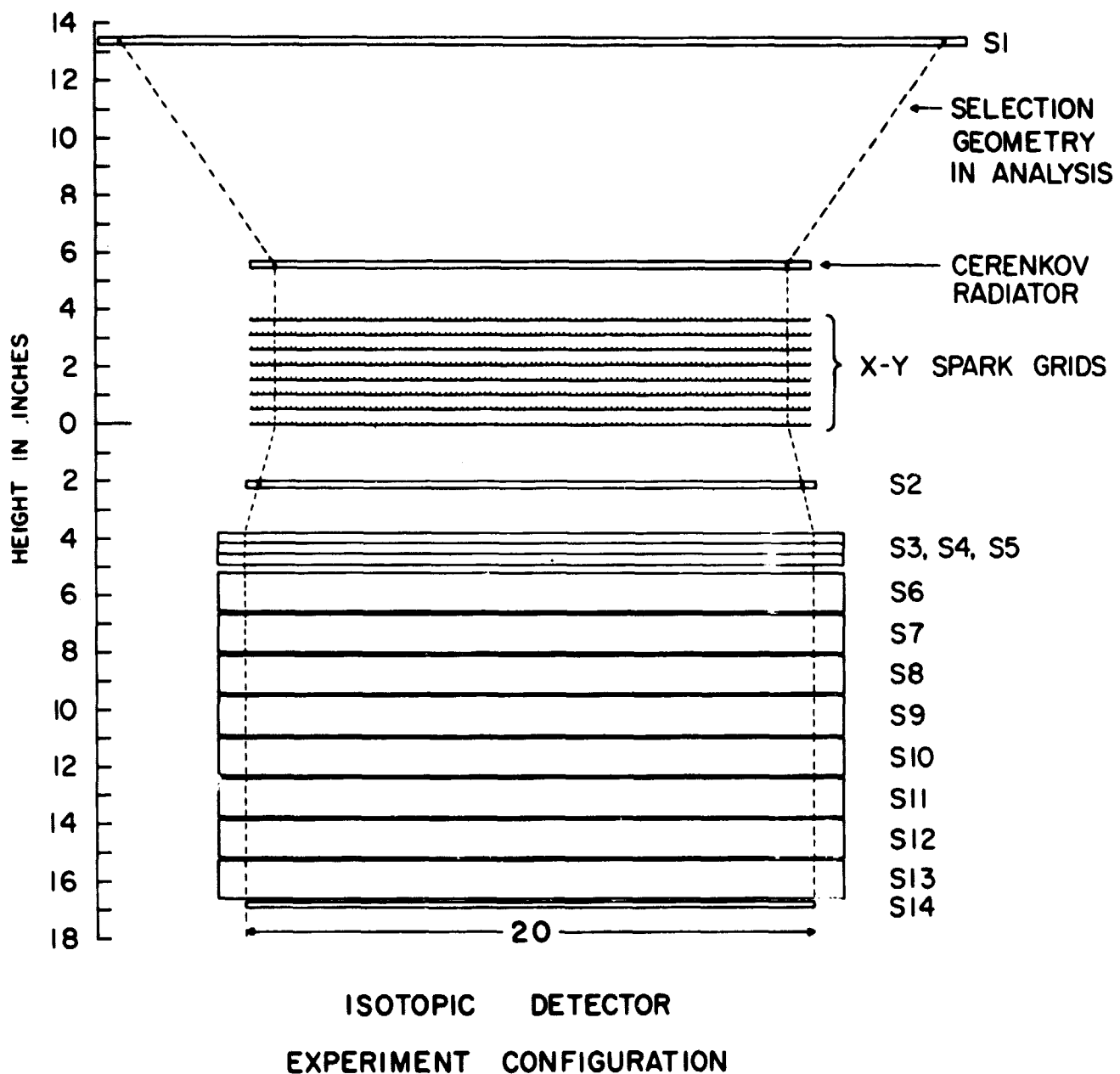
†Values in parentheses assume decay of Be-10, Al-26, Cl-36

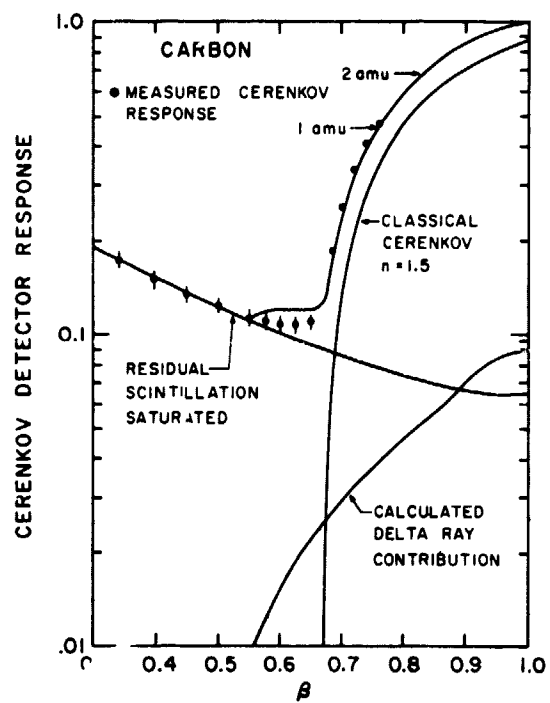
‡Recent cross section measurements (Lindstrom et al.) show an enhancement in nitrogen production not included in this formalism, hence this value (and some others such as Mn) may be somewhat high

TABLE III

CASE I		CASE II	
DATA	<u>SOLAR SYSTEM ABUNDANCES</u>	<u>^{20}Ne, ^{24}Mg, ^{26}Si, ^{23}Na, ^{27}Al</u>	SOURCE
F	19.0±.3	19.00	19.00
Ne	20.8±.1	20.47	20.32
Na	23.0±.3	23.00	23.00
Mg	24.3±.1	24.38-24.42*	24.09-24.14*
Al	26.6±.3	26.8-27.0*	26.8-27.0*
Si	28.1±.1	28.18	28.08

*Depending on ^{26}Al Decay





ORIGINAL PAGE IS
OF POOR QUALITY.

